Geochemical fingerprinting to determine sediment source contribution and improve contamination assessment in mining-impacted floodplains in the Philippines

Applied Geochemistry 159 (2023) 105808

Contents lists available at ScienceDirect

Applied Geochemistry

journal homepage: www.elsevier.com/locate/apgeochem

Geochemical fingerprinting to determine sediment source contribution and improve contamination assessment in mining-impacted floodplains in the Philippines

Justine Perry T. Domingo [a,b,*], Bryne T. Ngwenya [a], Mikaël Attal [a], Carlos Primo C. David [b], Simon M. Mudd [a]

[a] The University of Edinburgh, School of GeoSciences, Edinburgh, EH8 9XP, United Kingdom
[b] University of the Philippines, National Institute of Geological Sciences, Quezon City, 1101, Philippines

ARTICLE INFO

Editorial handling by Dr V Ettler

Keywords:
Apportionment
Provenance
Partitioning
Enrichment
Metals
Mining
Siltation

ABSTRACT

Constraining the main sediment sources and pathways across landscapes impacted by anthropogenic activity is essential to limit the dispersal of sediment-borne contaminants, especially in global conservation priority areas. This study examined the provenance, partitioning, and enrichment of metals in the floodplain of the mining-affected Santa Cruz catchment, The Philippines. Composite geochemical fingerprinting of fine sediment samples (n = 36) was performed using a stepwise statistical screening procedure (range test, Kruskal-Wallis H test, discriminant function analysis) to derive the optimum set of tracers. Using a standard unmixing model, flood deposits downstream of the mining areas were shown to be predominantly mining-induced (71.9 ± 7.7 %), followed by natural erosion from gullies and stream banks (15.1 ± 11.0 %) and agricultural sediment (13.0 ± 5.1 %). Element partitioning data (Log K_d = 1.3–6.6) during a high flow event indicated that metals are dominantly associated and transported via suspended particulate matter. Background concentrations of Ni and Cr were found to be orders of magnitude higher than the threshold values set by international sediment quality guidelines (SQGs), emphasizing the need for site-specific SQGs in mineralised areas. Enrichment factor values indicated low to significant contamination of flood deposits relative to natural and agricultural sediment (EF 1.0–5.5). Furthermore, it was demonstrated that using different conservative elements could considerably influence the enrichment factor calculation. Based on tracer screening tests, Th was shown to be the most suitable reference element. The findings provide new insights on the application of geochemical tracers in a mining setting and integrating fingerprinting approaches with traditional assessment techniques to improve the reliability of contamination risk assessment in other areas facing similar sediment pollution problems.

1. Introduction

Among the environmental issues linked to mining, the release of sediment from the mines to river systems can have the most detrimental impacts on water quality and river ecology (Kjelland et al., 2015; McIntyre et al., 2016). Such impacts are more pronounced in open-cast mines such as nickel laterite mining, which require removal of huge amounts of vegetation and overburden, producing highly erodible sediment at all stages of its operations (Bird et al., 1984; Apodaca et al., 2018). Mining areas in tropical regions are particularly vulnerable to intensified impacts due to hydrometeorological hazards (Holden, 2015); most of the annual sediment yield can be in fact generated by a single flooding event (Domingo et al., 2021). Overbank flows commonly occur in low-lying downstream areas during floods, leaving levee-type deposits of sand to mud-grained sediment on the floodplain as flood waters recede. These flood deposits could partially bury riparian vegetation and agricultural lands. In many areas around the world, these overbank deposits replenish the nutrients in the floodplains, resulting in more fertile soils for agriculture. However, floods can also transport metals and organic pollutants that typically exhibit strong affinity to fine sediment (Walling and Collins, 2016). Floodplains in historically mined watersheds can contain large quantities of metal-contaminated

* Corresponding author. University of the Philippines, National Institute of Geological Sciences, Quezon City, 1101, Philippines.
E-mail addresses: jptdomingo@nigs.upd.edu.ph (J.P.T. Domingo), bryne.ngwenya@ed.ac.uk (B.T. Ngwenya), mikael.attal@ed.ac.uk (M. Attal), cpdavid@nigs.upd.edu.ph (C.P.C. David), simon.m.mudd@ed.ac.uk (S.M. Mudd).

https://doi.org/10.1016/j.apgeochem.2023.105808
Received 7 August 2023; Received in revised form 27 September 2023; Accepted 13 October 2023
Available online 19 October 2023

sediment, which can be remobilised and/or undergo biogeochemical processing that may potentially yield more toxic forms of pollutants (Dennis et al., 2009; Lecce and Pavlowsky, 2014; Singer et al., 2016). Hence, the transport and deposition of fine sediment in river systems, farmlands, fishponds, and coastal areas have serious environmental implications that can persist well beyond the mining life cycle, which could ultimately outweigh the benefits of mining (Bai et al., 2011). Furthermore, background metal concentrations in mineralised areas can be naturally elevated, i.e., sediments eroded from gullies and channel banks may contain high metal concentrations. Thus, it is necessary to account for both anthropogenic and natural sediment sources.

In lieu of traditional measurement techniques such as sediment budgeting and using erosion pins/plots and profilometers, sediment fingerprinting has been successful in providing information on the provenance and contribution of different sediment sources (Collins and Walling, 2002). Sediment fingerprinting techniques rely on the assumption that sources possess one or more measurable properties that behave conservatively and that these properties can be used to distinguish one source from another (Collins et al., 2017). Applications of sediment fingerprinting include identifying primary sources within catchments, quantifying the relative contribution of these sources to the sediment yield, and examining the temporal and spatial variability of the source contributions (Palazón and Navas, 2017). Sediment fingerprinting can also provide additional information on sediment mobilisation processes such as surface (e.g., sheetwash) versus sub-surface erosion (e.g., gully, channel bank) and the spatial origin of sources (e.g., geology, land use) that would be difficult to access using other methods. With the wide range of available tracers, the suggested best practice is to examine multiple sets of properties to optimise the selection of the sediment fingerprint (Laceby et al., 2019). Although the behaviour of sediment tracers in a mining environment has not been widely studied, elemental geochemistry and geogenic radionuclides have been shown to differentiate between sediments from mining-affected tributaries and sediments coming from undisturbed areas (Sellier et al., 2020).

In addition to source provenance and apportionment, it is likewise important to determine the mode of contaminant transport, considering that metals are present in different forms and species in surface waters (Yang et al., 2014). There is a need to define whether contaminants are primarily transported downstream via particulates - from which a significant portion ends up temporarily deposited on the floodplain - or dissolved in the water column, which poses a greater bioavailability risk.

Understanding the main erosion processes and sources of contaminant-bearing sediment at the catchment scale is therefore crucial to effectively mitigate impacts (Macklin et al., 2006; Nosrati and Collins, 2019a). In the context of mining, being able to distinguish and disentangle the impacts of mining activities from other natural and anthropogenic pressures would allow for strategic intervention measures that could reduce ecological risks. This is especially important in tropical conservation priority areas that seek to expand mining activities for economic development, such as Indonesia and the Philippines – the top two nickel ore producers in the last 15 years (Brooks et al., 2006; Brown et al., 2016; Idoine et al., 2022). In this study, we aimed to: (1) quantify the relative contribution of different sediment sources to flood deposits in a mining-impacted catchment in the Philippines; (2) examine the primary mode of metal transport; and (3) assess the contamination and ecological risk posed by the flood deposits using existing pollution indices. Further to the purpose of source apportionment, we discuss how fingerprinting techniques can be integrated with traditional assessment approaches for an improved environmental risk evaluation.

2. Methodology

2.1. Study area

The Santa Cruz catchment (52.1 km^2) is situated in the municipality of Santa Cruz, Zambales province, on the western coast of Luzon Island, the Philippines (Fig. 1a). The climate is characterised by alternating dry and wet seasons: dry in November to April and wet in May to October. The mean annual rainfall in the catchment is estimated to be around 3500 mm, with maximum monthly rainfall in August, while January has the lowest rainfall. The mean annual temperature is 27.7 °C, being lowest in January at 26.7 °C and highest in April at 29.1 °C (data provided by the Philippine Atmospheric, Geophysical, and Astronomical Services Administration). Laterites and Quaternary alluvium cover 40 % and 28 % of the total catchment area, respectively; the former is extensive in the eastern part of the catchment, where the headwaters originate and where mining areas are concentrated, while the latter predominantly covers the western part of the catchment. The rest of the catchment is composed of harzburgites (17 %), pyroxenites (12 %), sandstone-shale units (3 %), and limestone (1 %) (Fig. 1b).

The main land uses are shrubland (61 % of catchment area) in the eastern/upstream portion followed by croplands (18 %) in the western/downstream portion of the catchment (Fig. 1c), consisting of grain crops (rice) and tree crops such as mango, coconut, and cashew. The rest of the catchment consists of grasslands (14 %), pasture (4 %), and woodlands (2 %). Although mining is not included in the different land use categories used by the state bureau (Bureau of Soils and Water Management, 2021), active mining areas and rehabilitation sites – hereafter referred to as disturbed areas – cover 5.86 km^2 or 11.3 % of the catchment. These disturbed areas, which include bare soil surfaces and siltation ponds, are well connected to the river network, especially as the main tributaries of the Santa Cruz River originate from this part of the catchment.

The nickel laterite deposit in Santa Cruz is a product of the intensive weathering of ultramafic units in the tropical Philippine climate. It is an oxide-type deposit with a typical laterite zonation consisting of limonite, saprolite, and bedrock (Fig. 2a). The Santa Cruz laterite unit is described by Aquino et al. (2022) in detail. The topmost limonite layer occurs as residual soil with a distinct red to yellow hue with high Fe and low Ni contents, while the limonite zone is further sub-divided into upper and lower zones. The upper limonite layer has reddish brown hue and mainly consists of poorly sorted, very fine grains (<1 mm) with medium to coarse fragments (5–10 mm) of Fe oxides (57–64 wt%), while the lower limonite has a brown-dark brown hue and has fine to coarse fragments (>10 mm) of Fe oxides (69–75 wt%) (Aquino et al., 2022). Significant concentrations of Ni (1.1–1.6 wt%), Mn (0.9 wt%), and Co (0.1 wt%) occur in the limonite zone, with concentrations that generally increase with depth. Underlying the limonite is the saprolite layer, which occurs as garnierite stringers and coatings on partially serpentinised peridotites with low Fe and high Ni contents. The saprolite is characterised by moderately to heavily weathered peridotite with yellowish-brown hue. In this layer, the Mg, Si, and Ni contents are highly enriched with 32–37 wt% Mg, 33–39 wt% Si, and 1.2 to 3.7 wt% Ni. Underneath, the bedrock comprises harzburgite with sporadic dunite lenses (Aquino et al., 2022). Typically, the upper limonite layer is stripped to allow extraction of the Ni-enriched layers underneath, generating large quantities of waste material. To retain material released from strip mining, numerous silt traps and siltation ponds are positioned across the mining tenements. In theory, these structures allow turbid runoff to decant before being discharged into the river network. The silt that has accumulated on these ponds is then dredged in the dry season and incorporated with the 'waste' material (i.e., the stripped upper limonite layer) to be used for rehabilitating the scarred landscape.

In 2022, eight out of the 29 nickel mines in the Philippines operate in Santa Cruz and extract nickel, chromite, and associated minerals (Mines and Geosciences Bureau, 2022). While natural erosion processes are also evident across the catchment in the form of landslides, gullies, and channel bank erosion (Fig. 2b–d), the inhabitants of Santa Cruz have become increasingly aware of the negative environmental impacts of nickel mining since large-scale operations started in the 2000s. Residents have noticed pronounced changes to the landscape in the form of deforested mountaintops and shallower streambeds; and in response to

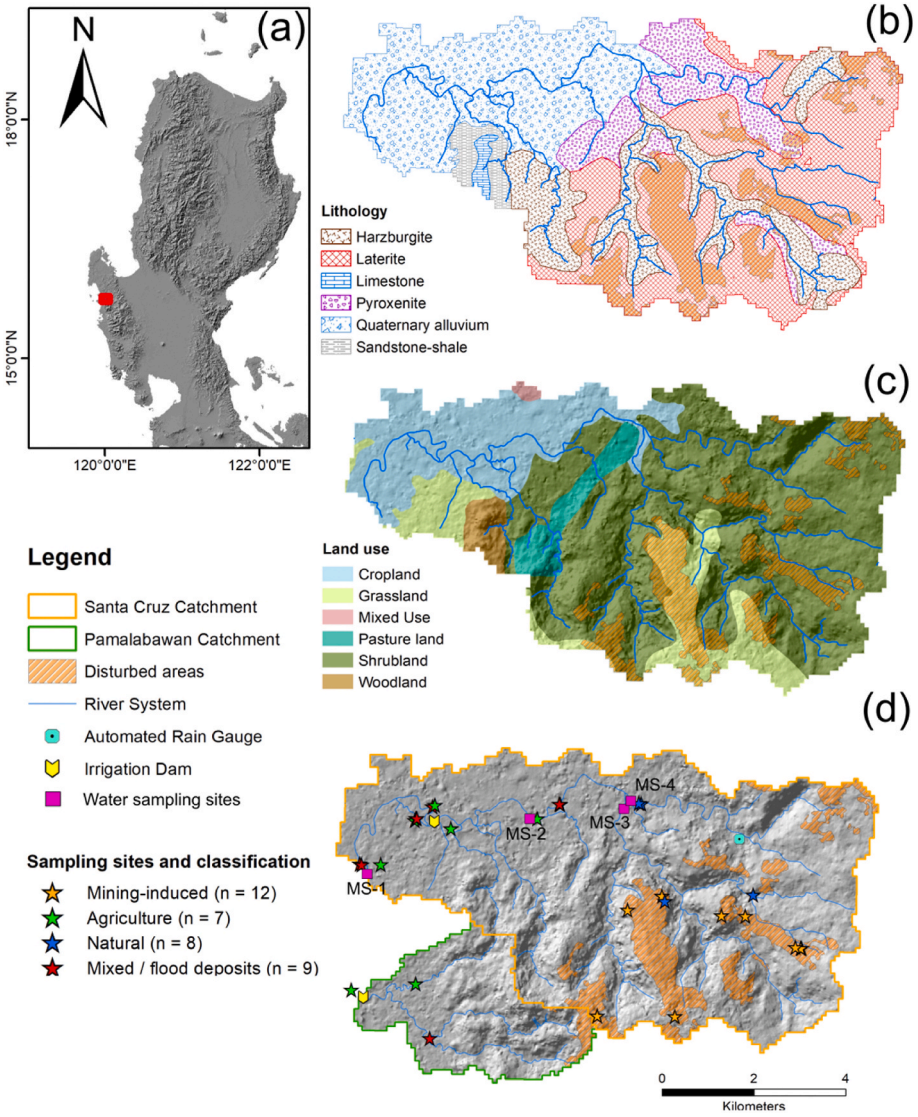

Fig. 1. (a) Location of the Santa Cruz catchment in Luzon Island, Philippines. Maps of the Santa Cruz catchment showing (b) lithologies, (c) land use types, and (d) collection sites of water samples and surface sediments from different origins (indicated by stars; see text for complete description). Samples collected in the adjacent Pamalabawan catchment is also shown. The location of the disturbed areas, i.e., active and rehabilitated mining sites, is shown on the maps as hatched areas in orange.

increasing complaints from locals against the mines, a multidisciplinary team composed of representatives from government agencies and non-governmental organisations was assembled in 2014 (Senate of the Philippines, 2014). Following the investigation of the mining operations, the government suspended four of the largest mines for employing unsystematic strip-mining methods that resulted in siltation in water bodies (Philippine Senate Blue Ribbon Committee, 2017). The following year, Typhoon Koppu generated widespread flooding and mudflows across Santa Cruz. Subsequently, the nickel mines that had their operations suspended since 2014 were blamed for the resulting degradation of the river system and reduced crop yields (Migo et al., 2018). To date, suspension orders for ore extraction and future expansion have been lifted after they demonstrated compliance with the environmental legislation set by the government (Clemente et al., 2018).

2.2. Data gathering and sampling

2.2.1. Hydro-sedimentary data

Precipitation and discharge data covering the period from June 2018 to July 2019 were collected at nine stations in the Santa Cruz Catchment and have been reported in Domingo et al. (2021). Precipitation was recorded using an automatic tipping-bucket installed in the upstream part of the catchment, while discharge was computed from the stage, which was recorded two to three times a day during the wet season.

2.2.2. Surface sediment sampling

Surface sediment samples (n = 36) were collected on 1st August 2018 from different sites in the mining areas and floodplain of the Santa Cruz catchment (Fig. 1d) to align source apportionment estimates with the corresponding spatial origin. The samples were classified under three types: (a) mining-induced (n = 12): sediment discharged from excavated hillslopes in active mining areas and from mine structures such as ore stockpiles, settling ponds, and rehabilitation areas; (b) natural (n = 8): sediment generated from natural sources within and outside mining areas such as gullies and stream banks; (c) agricultural (n = 7): sediment from croplands that are not known to be affected by overbank inundation; (d) flood deposits (n = 9): sediment that drapes riparian vegetation and croplands downstream following overbank flooding. The latter represent the siltation targeted for assessment of contamination in this study. Approximately 1 kg of sediment was collected from the top 15 cm

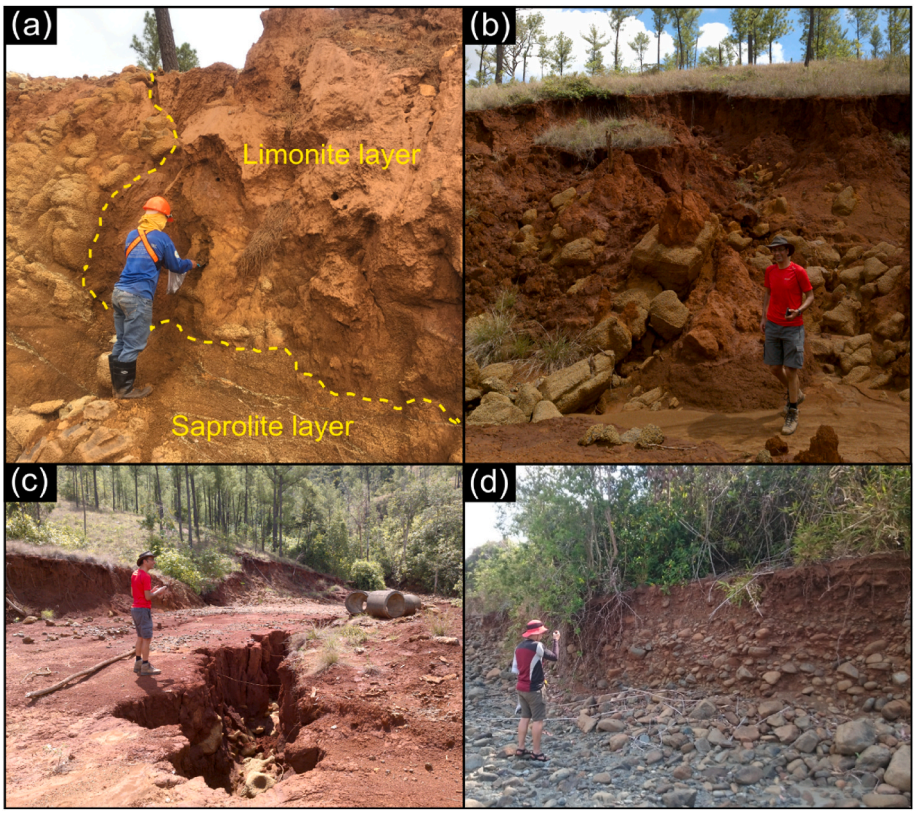

Fig. 2. (a) Typical profile of the nickel laterite deposit in the catchment showing an irregular contact between the limonite and saprolite layers, and irregular thickness with the saprolite exposed at the surface in places (bedrock not seen). Erosional features are extensive within and outside the mining tenements, including (b) landslides of a range of sizes, (c) gully erosion, and (d) channel bank erosion.

of a ~1 m^2 surface area per site, sealed in clean polyethylene bags, and stored at 4 °C.

2.2.3. *Water and suspended sediment sampling*

River water was sampled (n = 40) at four different sites of the Santa Cruz River: MS-1 at downstream, MS-2 at midstream, MS-3 and MS-4 at upstream sub-catchments (Fig. 1d). *In situ* water quality parameters including pH, temperature, conductivity, total dissolved solids (TDS), and oxidation-reduction potential (ORP) were measured using a calibrated handheld YSI multi-parameter water quality meter. Sampling was conducted on four separate dates to capture hydrologic variability: 28th June 2018, 10th July 2018, 22nd July 2018, and 1st August 2018. An additional set of water samples were collected at high flow on the 22nd July for total-recoverable metals. Fifty mL of each high-flow sample was transferred into sterile polypropylene tubes and centrifuged at 7000 rpm for 30 min. The residue was then acid-digested and analysed together with its supernatant to obtain the total-recoverable metal content. Meanwhile, the dissolved fraction was obtained by filtering the samples through a 0.45 μm membrane filter no later than 8 h after collection. Approximately 50 mL of the filtrate was used to rinse the PET bottles before storing the filtrate. Meanwhile, the particulate fraction was determined by the difference between the total-recoverable and filtered fractions (Nasrabadi et al., 2016). All samples were preserved by adding concentrated high-purity HNO_3 to a final pH of ~2 and stored at 4 °C prior to analysis.

2.3. *Sample pretreatment and analysis*

Surface sediment samples were oven dried at 103–105 °C for a minimum of 24 h. After drying, samples were disaggregated using a mortar and pestle, then sieved through a series of standard test sieves (1.7 mm, 250 μm, 125 μm, and 63 μm). The fine sediment fraction (<63 μm) was selected for the metals analysis due to its chemically reactive nature that makes it a significant conveyor of contaminants (Miller et al., 2015), and because of its relevance to the siltation problem (Apodaca et al., 2018). A sediment digestion procedure modified from McLaren et al. (1981) and McLaren et al. (1987) was adopted, wherein approximately 50 mg of each sample was weighed in Teflon tubes and digested by HNO_3–HCl–HF mixture (3 mL, 2 mL, and 0.5 mL, respectively) on a hot plate overnight at a temperature of ~100 °C. Perchloric acid was added onto a few samples to further assist digestion. The solutions were then diluted with 10 mL HNO_3 prior to analysis.

After acid digestion, the sediment samples (surface sediment + suspended sediment/residue from water samples) and water samples (filtered/dissolved fraction + supernatant from water samples) were analysed for major and trace elements (Al, Ba, Ca, Cd, Cr, Cu, Fe, K, Li, Mg, Mn, Na, Ni, P, Pb, Si, Sr, Ti, Zn), rare earth elements (Ce, Dy, Er, Eu, Gd, Ho, La, Lu, Nd, Pr, Sm, Tb, Tm, Yb), and radionuclides (Th, U) using Inductively Coupled Plasma-Optical Emission Spectrometer (Varian Visa Pro ICP-OES) and a high resolution Inductively Coupled Plasma-Mass Spectrometer (AttoM, HR-ICP-MS) at the Grant Institute, School of GeoSciences, University of Edinburgh, United Kingdom.

2.4. *Quality assurance and quality control*

Analytical data quality was ensured through standard operating procedures and quality assurance and quality control methods, including the use of calibration blanks and standards, reagent blanks, and duplicate samples. The precision and accuracy of the procedure was evaluated through recovery measurement of sediment certified reference material PACS-2 in duplicates, which showed mean recovery values of 99 % and 102 %. Details of the analytical measurements and the method detection limits are provided in Table A1 in the supplementary material.

Fig. 3. Box plots of major, trace, and rare earth element concentrations (in mg kg^{-1}) for sediment sources and flood deposits, with the median concentration indicated by the horizontal line. The numbers shown in the plots indicate the mean concentration for each source type. The elemental tracers that were excluded after each stage of stepwise screening procedure are also indicated.

2.5. Sediment geochemistry and fingerprinting

We assessed the use of major, trace, REEs, and radionuclides in the fine fraction of the surface sediment samples as potential tracers of sediment source areas for floodplain surface sediments. The fine sediment fraction is most commonly used in fingerprinting studies and has provided robust source discrimination for historical and contemporary sediments using geochemical tracers and mineral magnetic properties (Collins et al., 2016, 2017; D'Haen et al., 2012). We used the FingerPro package in R (Lizaga et al., 2020), which incorporates preliminary tests to select optimal tracers based on the two-step procedure proposed by Collins and Walling (2002) and uses a simple linear multivariate unmixing model to estimate the relative contribution of each sediment source. It has been successfully tested to identify sediment provenance with artificial samples (Gaspar et al., 2019).

2.5.1. Tracer conservation

Sediment fingerprinting studies typically use a simple screening technique called the range test to evaluate the conservative behavior of potential tracers (Collins et al., 2017). Accordingly, the range test was applied in this study, wherein elements in the flood deposits that fall outside the lowest and highest values in the sediment sources were excluded from subsequent analyses. The test ensures that the potential tracer values are within the values of the sources, indicating that major transformation has not occurred during sediment mobilisation and delivery, while tracers with values that fall outside the range could be considered non-conservative (Nosrati and Collins, 2019b; Palazón and Navas, 2017).

2.5.2. Sediment source discrimination

After non-conservative elements are removed from the suite of potential tracers, statistical tests are subsequently conducted for sediment source discrimination. In this study, the Kruskal-Wallis H-test (KW-H) and discriminant function analysis (DFA) were used for source discrimination. The KW-H was applied to determine which tracers differentiate the sediment sources by comparing median tracer concentrations of the sources at the 5 % confidence level (p-value = 0.05), and tracers that did not show significant difference between sources were excluded (Jalowska et al., 2017; Nosrati et al., 2018; Pulley et al., 2015). Subsequently, DFA was used to find the optimum source fingerprint, which consists of the minimum number of tracers that provides maximum discrimination between the sources (F-value = 0.1) (Palazón and Navas, 2017). This stepwise function selects tracers that minimize the Wilk's lambda value - a lambda value closer to zero indicates that variability within source types is reduced relative to the variability between source types (Lizaga et al., 2020; Palazón et al., 2015).

2.5.3. Source apportionment

Once the optimum source fingerprint was established, the relative contribution of each potential sediment source was determined using a standard linear multivariate mixing model in the FingerPro package:

$$\sum_{j=1}^{m} a_{i,j} \bullet \omega_j = b_i \tag{1}$$

which satisfies the following constraints:

$$\sum_{j=1}^{m} \omega_j = 1 \tag{2}$$

$$0 \le \omega_j \le 1 \tag{3}$$

where $a_{i,j}$ is the mean concentration of tracer i in sediment source j (j = 1 to m), ω_j is the relative weighting contribution of sediment source j, b_i is the concentration of tracer i (i = 1 to n) in the flood deposits, and m is the number of potential sediment sources (Lizaga et al., 2020). This procedure examines all possible combinations of each source contribution using Latin Hypercube Sampling (McKay et al., 1979) and the source proportions that conserve the mass balance for all tracers (Palazón et al., 2015). The goodness-of-fit (GOF) is calculated with the sum of squares of the relative error:

$$GOF = 1 - \frac{1}{n} x \left(\sum_{i=1}^{n} \frac{\left| b_i - \sum_{j=1}^{m} a_{i,j} \bullet \omega_j \right|}{\Delta_i} \right) \tag{4}$$

where Δ_i is the range of tracer i and n is the number of tracers selected (Lizaga et al., 2020). We then used the GOF to evaluate the quality of each candidate source combination. In this study, the number of samples used in the Latin Hypercube Sampling and the number of iterations were both set to 1000. The combinations that reproduced the flood sediment samples with the highest GOF from the best 1000 results were automatically selected.

2.6. Element partitioning

The partition coefficient K_d (in L kg^{-1}) between the particulate and dissolved form of each element was calculated given the equation:

$$K_d = \frac{C_s}{C_{aq}} \tag{5}$$

where C_s is the concentration of the metal in the solid phase and C_{aq} is the concentration in the dissolved fraction (in mg L^{-1}).

2.7. Contamination assessment

2.7.1. Sediment quality guidelines

A pre-mining historic database, which is needed to detect and attribute change, is almost non-existent in most mining areas worldwide (Zapico et al., 2017). Since there is no available sediment quality data in the Santa Cruz Catchment, we referred to sediments classified under the natural source type to represent background values that are not impacted/contaminated by mining activities or agricultural runoff.

Threshold values set by national or international agencies are typically used in environmental impact assessment studies, but since the Philippines does not have official sediment quality guidelines (SQGs), we used international SQGs from the following nations/organisations as reference: the Australian and New Zealand toxicant default guideline values for sediment quality (Commonwealth of Australia, 2019); the Canadian agricultural soil quality guidelines (Canadian Council of Ministers of the Environment, 2021); The Netherlands intervention values for sediment (Hin et al., 2010); the European Council maximum allowable concentration – environmental quality standards (The European Parliament and the Council of the European Union, 2008); the US National Oceanic and Atmospheric Administration sediment quality guidelines (1999); and the US Environmental Protection Agency freshwater sediment screening benchmarks (Pluta, 2006). Some SQGs have at least two designated values for pollutants: a lower threshold concentration in which biological effects are occasionally observed, and a higher threshold concentration wherein adverse biological effects frequently occur (Ke et al., 2017). We included the "default" and "high" guideline values of Australia and New Zealand, and the "low" and "median" effects range values of the US NOAA, which represent lower and higher threshold values, respectively, for the country/organization. The remaining SQGs used in the study have a single set of guideline values.

2.7.2. Enrichment factor

In addition to SQGs, different pollution indices were also used to

evaluate the degree of metal contamination in flood deposits in the downstream reaches of Santa Cruz River. One of the indices we used is the enrichment factor (EF), which adopts a normalisation approach for trace metal data to a variety of conservative elements. Using a fundamental assumption that the conservative elements have had a uniform flux from initial entrainment to deposition (Horowitz, 1991), this technique provides a reference for changes in the levels of other non-conservative elements. The EF of an element can be calculated by the following equation:

$$EF = \frac{\left(C^i/C^c\right)_{sample}}{\left(C^i/C^c\right)_{background}} \quad (6)$$

where $\left(C^i/C^c\right)_{sample}$ is the ratio of the concentration of the element i (C^i) to that of the conservative element c (C^c) in the sample, and $\left(C^i/C^c\right)_{background}$ is the same ratio in the background/reference sample. We used the average concentrations of the natural source type as background values.

Conservative lithogenic elements including Al, Fe, Th, and Ti have been used as reference elements for geochemical normalisation (Bern et al., 2019; Boës et al., 2011; Malvandi, 2017; Pekey, 2006; Varol, 2011). We calculated the EF using these elements as reference and adopted a five-category system to rank the degree of contamination (Sutherland, 2000):

EF < 2: Depletion to *minimal enrichment suggestive of no or minimal contamination*
EF 2–5: Moderate enrichment, suggestive of moderate contamination
EF 5–20: Significant enrichment, suggestive of a significant contamination signal
EF 20–40: Very highly enriched, indicating a very strong contamination signal
*EF > 40: Extremely enrich*ed, indicating an extreme contamination signal

2.7.3. Index of geoaccumulation

The index of geoaccumulation (I_{geo}) is another metric used to assess the environmental contamination status, given by the following equation:

$$I_{geo} = \log_2 \frac{(C^i)_{sample}}{1.5 \times (C^i)_{background}} \quad (7)$$

where $(C^i)_{sample}$ is the concentration of the element in the sample, $(C^i)_{background}$ is the background concentration of the element, and 1.5 is a correction factor due to lithogenic effects (Ke et al., 2017; Malvandi, 2017; Yang et al., 2014). Like the EF approach, the magnitude of pollution is assessed through ranking in the I_{geo} values:

$I_{geo} < 0$ *Unpolluted*
$0 < I_{geo} < 1$ *Unpolluted to moderately contaminated*
$1 < I_{geo} < 2$ *Moderately contaminated*
$2 < I_{geo} < 3$ *Moderate to strongly contaminated*
$3 < I_{geo} < 4$ *Strongly contaminated*
$4 < I_{geo} < 5$ *Strongly to extremely contaminated*
$I_{geo} < 5$ *Extremely contaminated*

2.7.4. Potential ecological risk index

The potential ecological risk index (PERI) is used to assess contamination levels and combine ecological and environmental effects with toxicology, consequently providing a more comprehensive assessment of potential ecological risk of the contaminant-bearing sediment (Ke et al., 2017). PERI is derived using the following equations:

$$PERI = \sum_{i=1}^{n} E_r^i \quad (8)$$

$$E_r^i = T_r^i \times CF_i \quad (9)$$

$$CF_i = \frac{C^i_{sample}}{C^i_{backIround}} \quad (10)$$

where CF_i is the contamination factor of element i, E_r^i is the potential risk index of the element, Ind T_r^i is the biological toxicity factor of the element as follows: Zn = 1; Cr = 2, Cu, Pb, Ni = 5; As = 10; Cd = 30. The PERI for the sediment is then calculated by summing up the risk indices of the abovementioned metals, which is categorized into five levels (Hakanson, 1980):

PERI < 150 *Low ecological risk*
150 < PERI < 300 *Moderate ecological risk*
300 < PERI < 600 *Considerable ecological risk*
PERI > 600 *Very high ecological risk*

3. Results and discussion

3.1. Sediment sources and metal concentrations

We examined the elemental concentrations in the sediment sources and flood deposits as a prerequisite to evaluating the contamination extent in the Santa Cruz Catchment (Table A2 in the supplementary material). Fig. 3 summarizes the mean elemental concentrations in flood deposits and various sediment sources in the catchment. We focused on six potentially toxic elements - metals that are considered as high priority in terms of pollution: Cd, Cr, Cu, Ni, Pb, and Zn (US Environmental Protection Agency, 2014). Due to their toxicity, non-degradability, and prolonged residence times, sediments that are enriched in these metals are considered hazardous (Pekey, 2006). Background metal concentrations are consistent with the local geology (Aquino et al., 2022), i.e., nickel laterite areas are characterised by inherently high Ni and Cr concentrations as observed in natural (and mining-induced) sediment (Fig. 3). Natural and mining-induced sediment exhibited the following mean concentration values, respectively: Ni (6,804 & 10,777 mg kg^{-1}) > Cr (5073 & 6144 mg kg^{-1}) > Zn (167 & 230 mg kg^{-1}) > Cu (58 & 82 mg kg^{-1}) > Cd (11 & 12 mg kg^{-1}) > Pb (6 & 5 mg kg^{-1}). In contrast, the agricultural source displayed considerably lower mean metal concentrations, with Ni and Cr at 2,141 mg kg^{-1} and 2,552 mg kg^{-1}, respectively. The mean concentration of some elements in the agricultural source type are significantly higher compared with other source types, such as Ca (18,960 mg kg^{-1}), K (1,099 mg kg^{-1}), and P (402 mg kg^{-1}), which are the main nutrients in chemical fertilizers widely applied for rice production. Metal concentrations in agricultural soils have been reported in previous studies in Santa Cruz and in other agricultural sites in the Philippines (Bacani and Farin, 2018; Domingo and Kyuma, 1983; Magahud et al., 2015). While the mean Cr concentration in agricultural sediment measured in the current study is higher than the reported Cr concentrations in previous studies, the Ni concentrations measured in this study are generally comparable (if not considerably lower) to previously reported values (Table A3 in the supplementary material). The deviation between the measured metal levels is presumably due to spatial and/or temporal differences in the sampling methodology. On a national scale, both Ni and Cr are more than a magnitude higher than the average range for Philippine rice soils (Domingo and Kyuma 1983; Magahud et al., 2015). It is important to note, however, that the previous studies used different grain size fractions, while our study focused on the finest sediment fraction (<63 μm) due to its relevance to siltation.

The examination of flood deposits is particularly important due to the potential contamination of agricultural land downstream of the

mining tenements, which occurs through overbank deposition of fine lateritic mud during floods. Flood sediment samples generally exhibited lower mean concentrations in metals compared with the mining-induced and natural sediment sources, particularly Ni and Cr (5,045 mg kg^{-1} and 3,064 mg kg^{-1}, respectively.)

3.2. Sediment contribution of mining vs. non-mining sources

Sediment fingerprinting identifies different sediment sources in the catchment through a distinct set of intrinsic properties – the so-called 'fingerprint'. The procedure essentially involves two steps: first is the identification of a set of sediment-associated geochemical parameters that can be utilised to distinguish between variously defined sources, and second is the comparison of the geochemical parameters to estimate relative proportion of sediment coming from each of the identified sources (Miller et al., 2015). Composite geochemical fingerprinting has been successfully used for identifying whether sediments were derived from mining or non-mining tributaries (Sellier et al., 2020).

In this study, we used the fingerprinting approach to derive a geochemical signature that distinguishes mining-induced sediment (from active and rehabilitated mining areas and structures) from other sources within and outside mining areas, i.e., natural sediment from gully and channel bank erosion, and agricultural sediment. From the suite of elements considered as potential tracers, 16 out of 35 elements were deemed to be non-conservative based on the range test and were excluded from analyses. Subsequently, the KW-H test showed no significant difference in the median concentrations of six elements, which further narrowed down the potential tracers to 13 elements. The stepwise DFA removed three elements from consideration, indicating an optimum source fingerprint comprised of 10 elements: Ca, K, Li, Na, Ni, P, Sr, Ce, Th, and U (Fig. 3). The resulting biplots from the DFA confirmed that the set of tracers can sufficiently distinguish between source types (Fig. 4).

The results of the unmixing process using the source variability of the best 1000 results are shown in Fig. 5. Using the mean source contributions from the mixed samples, the flood deposits over the low-lying floodplains downstream of the mining areas were shown to be predominantly composed of sediments derived from mining disturbance (71.9 ± 7.7 %), with contribution from natural sources (15.1 ± 11.0 %)

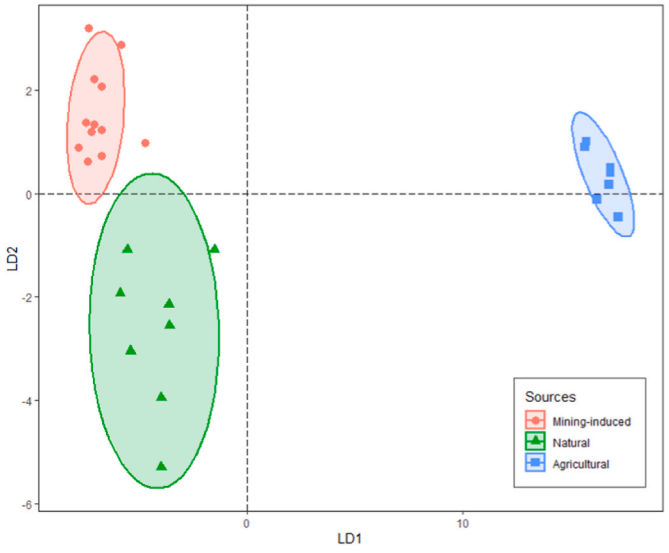

Fig. 4. Biplot of the discriminant function analysis (DFA) results showing separate clusters representing different sediment source types. LD1 and LD2 represent the groupings of predictor variables which provide the best discrimination between sediment sources as indicated by the horizontal and vertical linear boundaries.

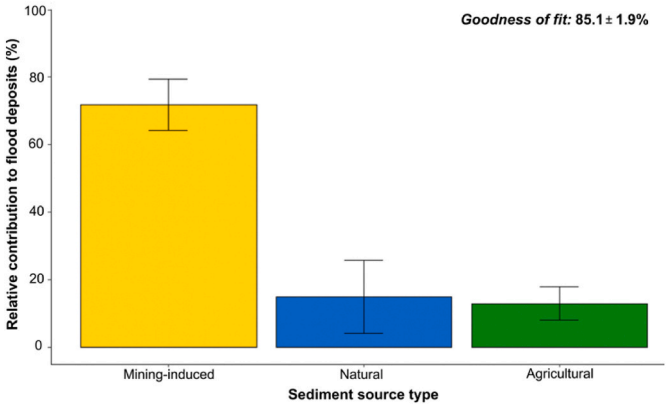

Fig. 5. Results of unmixing model showing the relative contribution of each sediment source to the flood deposits sampled in the Santa Cruz catchment.

and agricultural outflow (13.0 ± 5.1 %). These results indicate that, on average, active mining areas and rehabilitation sites in the Santa Cruz Catchment (which cover 11 % of the catchment area) contributed approximately 72 % of the sediment that was transported and deposited on floodplains, and eventually delivered to the ocean. These numbers are comparable with the findings of Sellier et al. (2020) who demonstrated that tributaries draining active and abandoned nickel mining areas, which cover 21 % of the total catchment area of the Thio River, New Caledonia, contributed between 63–82 % and 84–86 % of the sediment supply to the estuary during two separate flood events.

Our results provide new insight on the behaviour of geochemical tracers in a mining environment, particularly for nickel laterite areas (Sellier et al., 2020), with select elements exhibiting source-to-sink conservatism with distinct concentrations that allow them to represent different sediment sources in the catchment. This potentially presents an improvement from the composite fingerprinting approach reported in mining areas (e.g., Sellier et al., 2020), in which the sediment contribution from specific spatial sources or land-use types can be differentiated and quantified (e.g., mining-derived, natural, agricultural) as opposed to a general classification between mining and non-mining sources only. Hence, the set of geochemical tracers identified and used in the study may also be considered in future fingerprinting studies in nickel laterite regions for better sediment source discrimination.

In addition, our data provide further evidence that a large proportion of sediments can originate from disturbed areas that cover small fractions of the catchment area, consequently emphasizing the need to focus remediation work on erosion hotspots (Messina and Biggs, 2016). Similar observations were made in other regions with significant land disturbance not limited to mining areas. For instance, the US Geological Survey reported that in the Kawela watershed in Molokai, Hawaii, the volcanic soils disturbed by grazing that make up less than 5 % of the catchment area have produced most of the sediment exported by the river; of that 5 %, around 1 % produces approximately 50 % of the sediment (Risk, 2014; Stock et al., 2010). This phenomenon was also observed in St. John in the U.S. Virgin Islands, where unpaved roads were the dominant sediment source. Although these roads covered only 0.3–0.9 % of the catchment, they contributed to the sediment yield as much as 5–9 times compared to undisturbed portions (Ramos-Scharrón and MacDonald, 2007).

3.3. Mode of contaminant transport

The next research question we aimed to address in this study relates to the dominant mode of metal transport. The element partition data derived from the particulate and dissolved concentrations measured in the high flow samples (Table A4 in the supplementary material) indicated that elements are predominantly associated with the particulate

fraction during a high flow event in Santa Cruz River, with very low dissolved concentrations for most of the elements (Fig. 6). Among the elements examined, Mg exhibited the highest dissolved concentrations relative to the particulate fraction. We also noted an increase in the dissolved concentrations of Ca, K, and Na from upstream to downstream of the catchment, that could be linked with the presence of agricultural lands in the vicinity of the most downstream station MS-1. Another possible cause is the tidal backflow that regularly occurs at the site manifested by a significantly higher salinity - at least three times higher than the rest of the stations (Table A5 in the supplementary material). Nonetheless, the particulate concentrations of all elements are at least two orders of magnitude higher than the dissolved fraction.

We calculated the partition coefficient (K_d) – a measure of the affinity of the element between the water and the sediment at equilibrium conditions (Miller and Miller, 2007) – to further examine metal mobility in the system. The K_d value can been used to understand the behaviour and fate of metals in mine waters (e.g., Jung et al., 2005), where higher K_d indicates preferential association and enrichment of metals in the sediment (i.e., low geochemical mobility), while lower K_d suggests high availability and mobility in the water for biological uptake. Table 1 shows the Log K_d values of each element compared to the median K_d values from different freshwater systems worldwide (Sheppard et al., 2009). Excluding REEs, the relatively high K_d values measured in the Santa Cruz River during a high flow event indicates preferential retention of metals in sediment particles. In addition, the elements mostly displayed K_d values within two orders of magnitude of the median K_d values in literature. The significant difference in K_d values could be expected since K_d is highly dependent on the system and conditions in which they are measured, hence site-specific measurements could be different from global values reported in other areas (Sheppard et al., 2009). Even adjacent systems can exhibit significantly different behaviours, such as the Mersey and Humber rivers in England which showed K_d values varying by an order of magnitude (Comber et al., 1995). Hence, using generic K_d values found in literature could lead to significant errors in predicting the impacts of contaminant transport in a particular system; for this reason, K_d values measured at site-specific conditions should be used instead (US Environmental Protection Agency, 1999).

Among the four sampling sites, the most downstream station MS-1 exhibited the lowest levels of dissolved concentrations as shown by the number of undefined values, i.e., dissolved concentrations are below detection limit particularly for REEs (Table A5). In terms of metal mobility, the following order was observed: Ni > Cr > Cu > Pb. K_d values of Cd and Zn cannot be determined due to low levels of dissolved concentrations of the two elements, which essentially implies K_d approaching infinity and therefore even more particle transported. The order of metal mobility observed in the Santa Cruz Catchment is comparable with observations in the Yangtze River catchment in China, i.e., Cd > Cu > Pb (Zhao et al., 2013), and in the Shadegan Wetland in Iran, i.e., Ni > Pb > Zn (Yavar Ashayeri and Keshavarzi, 2019). In contrast, Jung et al. (2005) reported a reversed order of mobility in the Kwangyang mine area, Korea (Pb > Zn > Ni=Cd). These differences underpin the role of different factors unique to each site such as pH and salinity, which are both key controls in the adsorption and dissolution of metals in the environment (Gäbler, 1997; Acosta et al., 2011; Zhao et al., 2013; Król et al., 2020). Since the Santa Cruz River had maintained a neutral pH during the sampling campaign (Table A5), we presume no pH-induced changes in the metal mobility. On the other hand, the salinity increase at the downstream station MS-1 may increase the availability of metals for uptake, especially Cd due to competition with other cations for sorption sites (Acosta et al., 2011; Zhao et al., 2013). It is worth noting that aside from sorption, there are other mechanisms that influence metal distribution between the particulate and dissolved phases. For less conservative metals such as Fe and Al, redox and precipitation processes can form Fe and Al hydroxides (Herzog et al., 2020; Mora et al., 2017; Nordstrom and Ball, 1986), which may significantly contribute to suspended sediment concentrations especially in mining-impacted areas with high background metal concentrations like the Santa Cruz catchment.

On the whole, the element partitioning data are in agreement with previous studies which suggest that metal contaminants are usually associated with particulates that are transported and deposited downstream (Balaban et al., 2015; Macklin et al., 2006). Considering that water sampling was conducted during a flood event, the upsurge in the suspended sediment could have resulted to a higher particulate-dissolved ratio, which, in effect diluted the dissolved fraction (Wen et al., 2013). By demonstrating that metal transport in Santa Cruz is controlled by the particulate fraction, we emphasize that the key to limiting the risk of metal contamination lies in the management of suspended sediment transport. We also recommend conducting studies that further examine the role of environmental variables such as changing hydrologic seasons, tides and metal speciation in the partitioning behaviour, as these factors have not been widely studied (Feng et al., 2017). Such analyses are crucial to better understand the mobility and bioavailability of these contaminants in the system.

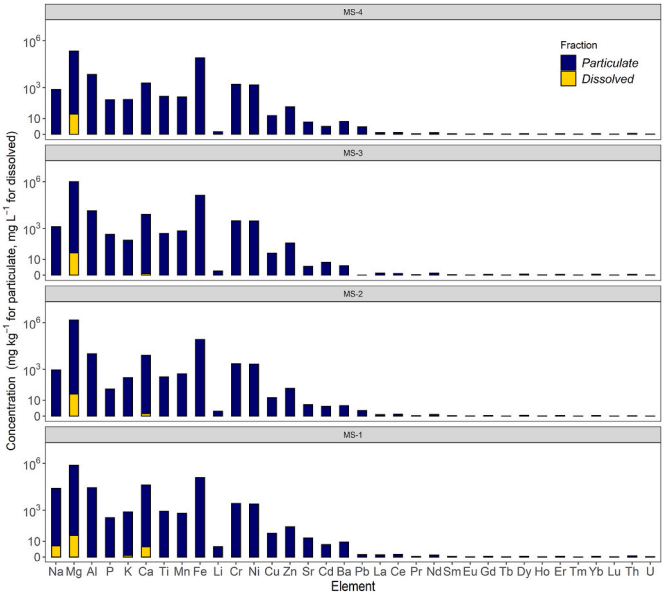

Fig. 6. Particulate vs dissolved elemental concentrations in water samples collected during a high flow event (22nd July 2018) from upstream (MS-4) to downstream (MS-1).

3.4. Extent of contamination in the Santa Cruz catchment

3.4.1. Sediment quality guidelines

Due to the absence of national SQGs in the Philippines, the flood deposits and sediment sources were compared with various international SQGs instead, which provide a simple way to evaluate the degree to which the contaminant-bearing sediments might adversely affect the aquatic ecosystem (MacDonald et al., 2000). In addition, we used the natural source type as reference/baseline values. Fig. 7 shows the background concentrations in the study area as compared with sediment quality guidelines. The mean concentrations of Ni and Cr greatly exceeded all the SQGs used. The largest differences between actual values and permissible limits are seen with Ni, wherein Ni levels in mining and natural source types and flood sediment samples are more than one order of magnitude higher than the maximum permissible limit of 210 mg kg^{-1}, while the Ni content in agricultural sediment is still two times greater than the maximum guideline value. Similarly, mean Cr concentrations in the sediment sources and flood deposits exceeded SQG values, including agricultural sediment that is the lowest among source

Table 1
Comparison of partition coefficient values (Log K_d) obtained in the current study and in literature, i.e., median K_d values from different freshwater systems extrapolated from > 130 publications by Sheppard et al. (2009).

Site	Mn	Fe	Cr	Ni	Sr	Pb	La	Nd	Sm	Ho	Tm	Yb	Th	U
Santa Cruz River *(this study)*	5.3–5.4	6.3–6.6	4.9–5.4	5.3–5.4	3.2–4.6	3.0–3.8	2.0–3.2	2.6–3.1	2.8–3.2	2.7–3.3	2.9–3.4	2.9–4.2	3.7	1.3
Literature-based values	4.4	5.2	4.6	3.2	2.7	5.1	5.5	5.9	5.6	5.4	5.3	5.5	4.9	4.2

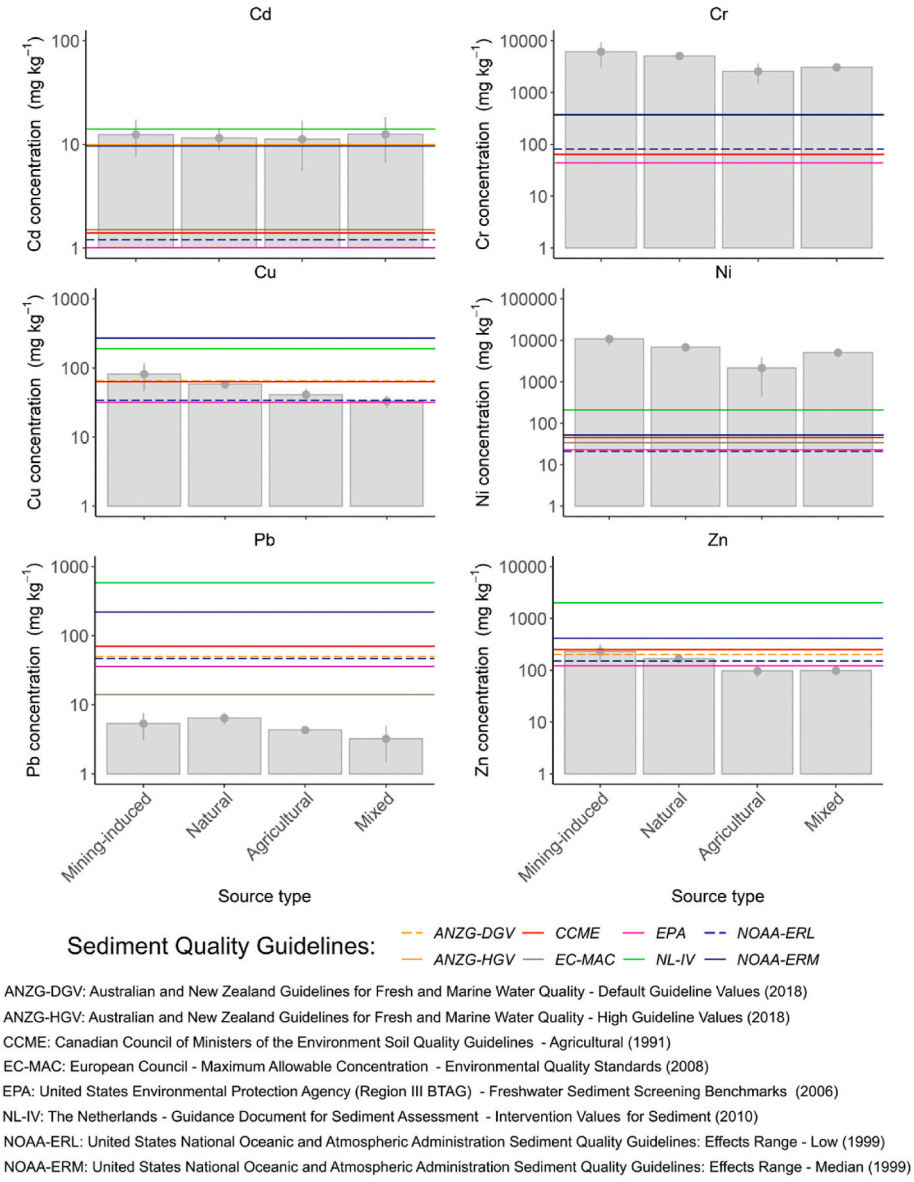

Fig. 7. Metal concentrations in sediment source types and flood deposits compared with sediment quality guidelines, with the dashed lines representing "lower" threshold values (i.e., ANZG Default Guideline Values and NOAA Effects Range-Low) and solid lines indicating "higher" guideline values. Values under the natural source type are considered as baseline values in the study area.

types but is four times higher than the maximum threshold concentration (370 mg kg^{-1}). For Cd, all source types and flood sediment samples exceeded the minimum guideline (1.2 mg kg^{-1}) but only the mining-induced sediment exceeded the maximum guideline (14 mg kg^{-1}). For Cu, all source types and flood deposits exceeded the minimum threshold value (34 mg kg^{-1}) but all are below the maximum threshold value (270 mg kg^{-1}). For Zn, only the mining and natural source types exceeded the minimum limit (121 mg kg^{-1}) but they are far below the maximum limit (2000 mg kg^{-1}). Lastly, mean Pb levels in all source types and in the flood sediment samples are significantly below the minimum guideline value (14 mg kg^{-1}). Although these results are somehow expected for lateritic sediments that are naturally metal-enriched, it is concerning for agricultural sediment to exhibit very high metal content. Most noteworthy are the mean Ni and Cr levels in samples that exceeded maximum SQG values, which could potentially increase risks to bioaccumulation and toxicity. In addition, the results highlight that using generic SQGs may not be always suitable due to differences in geologic setting where background values could be orders of magnitude greater than (inter)national threshold values. In cases such as this, site-specific guidelines are better suited to develop

contamination assessment and management procedures.

3.4.2. Pollution indices

Different pollution indices were also used to assess the extent of contamination in flood deposits in the Santa Cruz catchment. Among several indices used in pollution studies, EF has been considered as superior for contamination assessment since the normalisation element identifies anthropogenic influence and detects changes in sedimentary composition (Duodu et al., 2017; Hu et al., 2015). Here we calculated the EF of priority metals with respect to natural, agricultural, and mining-induced source; the latter was included since it could be considered as not anthropogenically modified (but anthropogenically induced). We used Al, Fe, Th, and Ti as reference elements, which have been widely used in pollution studies due to their apparent conservative behaviour (Bern et al., 2019; Boës et al., 2011; Malvandi, 2017; Pekey, 2006; Varol, 2011). While I_{geo} and PERI values indicated no contamination and low potential ecological risk ($I_{geo} < 0$; PERI < 150), EF values showed low to moderate enrichment with respect to natural sediment (EF = 1.1–3.7), and low to significant enrichment with respect to agricultural sediment (EF = 1.0–5.5) (Table 2). It is important to note that these values are more indicative of high background metal concentrations than of the actual contamination level. In this case, the agricultural sediment may serve as a more appropriate reference to assess the actual contamination considering the recurring deposition of fine sediment on croplands during flood events. Furthermore, the biogeochemical processing of metals in the floodplain needs to be examined to further understand the potential ecotoxicity of the contaminant-laden sediment to the ecosystem (Singer et al., 2016). These findings underscore a more cautious approach in relating pollution indices to contamination signal and pollution risk, especially in mineralised areas where metal concentrations are naturally elevated.

3.4.3. Sediment fingerprint as a guide for enrichment factor calculation

We observed considerable variability in the resulting EF values depending on the reference element used. Relative to natural sediment, all the reference elements suggested minimal to moderate enrichment (Fig. 8a); in contrast, the enrichment signal can range from minimal to significant for the same metal when the agricultural sediment is used as reference (Fig. 8b). The sensitivity of the enrichment factor approach is considerably influenced by the geochemical composition of the reference and target samples, wherein a greater compositional difference between the reference and target sediment leads to higher variability of the enrichment factor calculations. Subsequently, this observed discrepancy could lead to an inaccurate assessment of the actual contamination status of an area. The precision of the calculations may then be improved by selecting a conservative reference element that best distinguishes the reference material, if applicable.

To address this, we integrated sediment fingerprinting to guide the selection of the most appropriate reference element. Based on the result of the range test (Fig. 3), Al, Fe, and Ti can be excluded as reference since these three elements did not pass the conservation test. This result is consistent with previous studies showing non-conservative behaviour of Fe and Al under certain conditions, e.g., circum-neutral pH and/or higher salinity levels can result in the precipitation of Fe and Al hydroxides (Herzog et al., 2020; Mora et al., 2017; Nordstrom and Ball, 1986). These conditions were observed in the Santa Cruz catchment (Table A5), and the high background metal concentrations may likewise promote the formation of such hydroxides. As an additional test, KW-H and DFA were independently performed on the elemental data; likewise, only Th passed both statistical tests among the four reference elements (Table A6 in the supplementary material).

As a final test, we applied principal component analysis (PCA) to the resulting set of tracers from KW-H and DFA to identify the elements that best distinguish between and represent the sediment source types (Bern et al., 2019; Zhang et al., 2018). Initially, PCA was performed using the original fingerprint used for source apportionment (discussed in Section 3.2). The resulting principal components explained 65.9 % and 16.1 % of the variance (Fig. 9a). Using more stringent critical values for KW-H and DFA (i.e., p-value = 0.01 and F-value = 0.01, respectively), the resulting biplot showed only Ca, Th, and U with two principal components explaining 65.3 % and 26.0 % of the total variance (Fig. 9b). Based on the PCA results, the tracers that best distinguished the different sediment sources are the following: Ni for mining-induced sediment, Th and U for natural sources, and Ca for agricultural sediment. Accordingly, the highest concentration of these elements were also observed in the corresponding sediment source type (Fig. 3). This result is expected since Ni is most enriched in active mining areas, whereas Ca is one of the common nutrients found and applied in agricultural soil. For natural sediment sources, the result could be due to the characteristic depletion of Th and U in peridotite massifs where nickel laterite ores are extracted, in contrast with the natural enrichment of these elements in volcano-sedimentary units (Sellier et al., 2020). These two elements were previously identified as tracers that can distinguish sediment contributions between tributaries with and without nickel mining activities. Taken together, the results suggest that Th is the most appropriate reference element among the four conservative elements initially considered for the calculation of enrichment factors in the catchment.

Overall, the findings indicate that nickel mining activities, which have long been presumed to aggravate siltation in the Santa Cruz Catchment, indeed play a dominant role as most of the metal-laden sediment deposited on the floodplain during inundation originated from active mining areas. Accordingly, the metals adsorbed onto the floodplain sediments are mostly discharged from the mine sites at the onset of the wet season when suspended sediment concentration is at its highest due to the flushing effect (Domingo et al., 2021). As these sediments can cause moderate to significant contamination, priority should be given on the proper containment and management of sediments within the mining areas to limit other negative impacts associated with excessive sedimentation in the river system and coastal areas. Importantly, it was illustrated how sediment fingerprinting can provide new perspectives that could guide in the selection of the reference element for enrichment factor calculations and improve the reliability of the contamination assessment.

4. Conclusion

This study presents an integrated assessment of the sediment source contribution and degree of floodplain contamination in a nickel-mining affected catchment in the Philippines. Examination of the metal levels across the Santa Cruz catchment revealed that background concentrations are naturally high, with Ni and Cr concentrations that are orders of magnitude higher than the sediment quality guidelines used in the

Table 2
Range of (a) enrichment factor (EF) of selected metals in the flood deposits relative to the different source types, calculated using different reference elements: Al, Fe, Th, Ti; (b) index of geoaccumulation (I_{geo}); (c) potential ecological risk index (PERI).

Source type	(a) EF						(b) I_{geo}						(c) PERI
	Cd	Cr	Cu	Ni	Pb	Zn	Cd	Cr	Cu	Ni	Pb	Zn	
Mining-induced	0.5–2.1	0.3–1.0	0.2–0.8	0.3–1.0	0.3–1.2	0.2–0.9	−0.6	−1.6	−1.9	−1.7	−1.3	−1.8	39.0
Natural	1.1–3.2	1.1–3.3	1.1–3.4	1.1–3.5	1.1–3.6	1.1–3.7	−0.5	−1.3	−1.4	−1.0	−1.6	−1.4	43.5
Agricultural	1.0–5.0	1.0–5.1	1.0–5.2	1.0–5.3	1.0–5.4	1.0–5.5	−0.4	−0.3	−0.9	−0.7	−1.0	−0.6	56.3

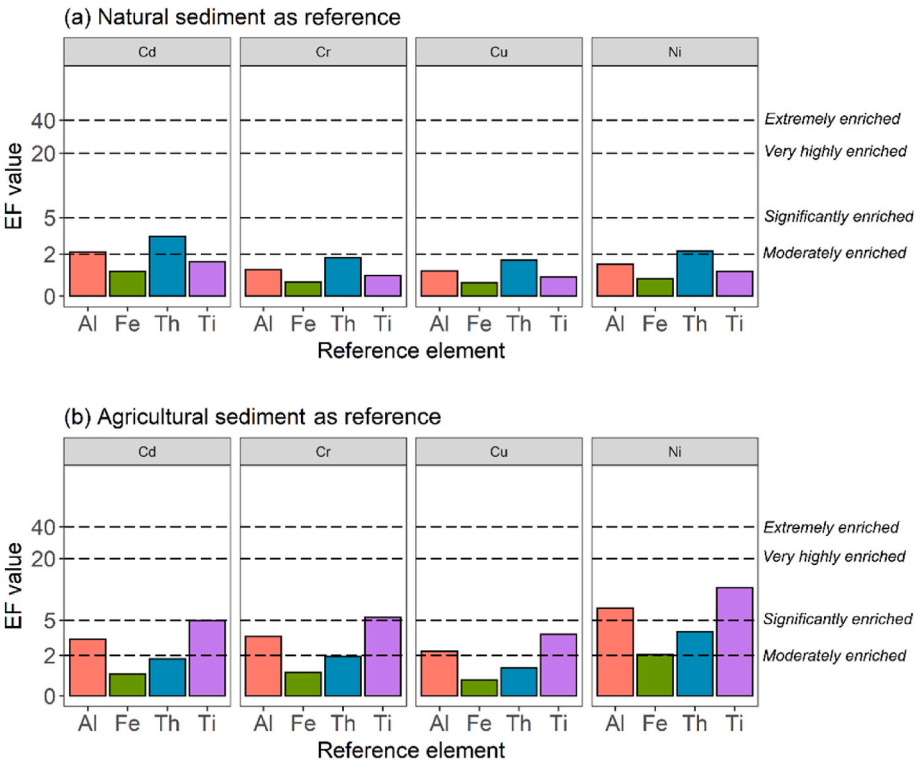

Fig. 8. Comparison of enrichment factors (EF) in flood deposits calculated using different conservative elements with (a) natural sediment source (b) agricultural sediment source as reference, showing the variability of the enrichment factors depending on the reference material and conservative element used in the calculations.

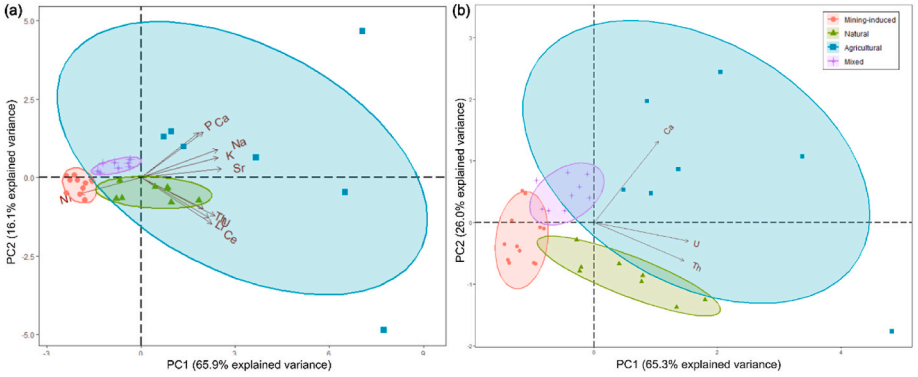

Fig. 9. (a) Biplot of the principal components analysis (PCA) of the original composite fingerprint derived using the default critical values in KW-H test and DFA; (b) resulting principal components derived using more stringent critical values in KW-H test and DFA. The direction of arrows indicates the elements that best distinguish the sediment source types.

study.

We explored the use of sediment fingerprinting with different sets of potential tracers to discriminate spatial origins in a nickel mining catchment. We found that a geochemical fingerprint (Ca, Ce, K, Li, Na, Ni, P, Sr, Th, and U) statistically differentiates mining, natural, and agricultural sediment. Using an unmixing model, we showed that approximately 72 ± 8 % of flood sediment deposited on the floodplains is mining-derived. In addition, K_d values indicated that metals are primarily transported via the particulate fraction during a flood event, which means that the risk of metal contamination may be minimized by limiting sediment-laden runoff from the mine sites.

Due to high background metal concentrations, the I_{geo} and PERI values suggested low contamination and potential ecological risk compared in flood deposits relative to natural sediments. However, EF values indicated moderate to significant metal enrichment, particularly with respect to agricultural sediment. We showed how enrichment factor calculations are highly dependent on the reference element used, and that sediment fingerprinting can provide the additional perspective to allow for a more reliable assessment of the actual contamination status. It is highly recommended to conduct proactive rehabilitation of floodplain and riparian zones to minimise the potential ecotoxicity of contaminated sediments. To solve the longstanding siltation problem downstream of nickel laterite mining areas, the enhancement and upkeep of mine environmental structures should be prioritised. The integrated sediment fingerprinting approach outlined in this study can prove useful in other areas facing similar sediment pollution problems.

Declaration of competing interest

The authors declare that they have no known competing financial

interests or personal relationships that could have appeared to influence the work reported in this paper.

Data availability

Supplementary material is provided with the manuscript.

Acknowledgements

This work was funded by the British Council and the Department of Science and Technology - Science Education Institute through the DOST-Newton PhD Scholarship awarded to Justine Domingo (Grant Number 279692019), with additional financial support from the University of Edinburgh through a Moray Endowment Fund Award and a Research Development Fund Award (School of GeoSciences). The authors would like to thank the mining companies in Santa Cruz that allowed access to their mining tenements and assisted in the collection of sediment samples. Special thanks to the Environment Monitoring Laboratory, Earth Materials Science Laboratory, and Nannoworks Laboratory (University of the Philippines – National Institute of Geological Sciences), and to the Philippine Nuclear Research Institute - Nuclear Materials Research Section for the use of facilities and equipment for sample preparation; to Dr. Laetitia Pichevin, Dr. Gavin Sim, and Mr. Steve Mowbray from the School of GeoSciences for assisting with the laboratory analyses.

Appendix A. Supplementary data

Supplementary data to this article can be found online at https://doi.org/10.1016/j.apgeochem.2023.105808.

References

Acosta, J.A., Jansen, B., Kalbitz, K., Faz, A., Martínez-Martínez, S., 2011. Salinity increases mobility of heavy metals in soils. Chemosphere 85, 1318–1324. https://doi.org/10.1016/j.chemosphere.2011.07.046.

Apodaca, D.C., Domingo, J.P.T., David, C.P.C., David, S.D., 2018. Siltation load contribution of nickel laterite mining on the coastal water quality of Hinadkaban Bay, Surigao Provinces, Philippines. IOP Conf. Ser. Earth Environ. Sci. 191 https://doi.org/10.1088/1755-1315/191/1/012048.

Aquino, K.A., Arcilla, C.A., Schardt, C., Tupaz, C.A.J., 2022. Mineralogical and geochemical characterization of the Sta. Cruz nickel laterite deposit, Zambales, Philippines. Minerals 12. https://doi.org/10.3390/min12030305.

Bacani, M.R.B., Farin, A.N., 2018. Assessment of heavy metals in agricultural crops near mining areas in Zambales, Philippines. Nat. Environ. Pollut. Technol. 17, 869–876.

Bai, Y., Wang, R., Jin, J., 2011. Water eco-service assessment and compensation in a coal mining region - a case study in the Mentougou District in Beijing. Ecol. Complex. 8, 144–152. https://doi.org/10.1016/j.ecocom.2011.01.003.

Balaban, S.I., Hudson-Edwards, K.A., Miller, J.R., 2015. A GIS-based method for evaluating sediment storage and transport in large mining-affected river systems. Environ. Earth Sci. 74, 4685–4698. https://doi.org/10.1007/s12665-015-4440-5.

Bern, C.R., Walton-Day, K., Naftz, D.L., 2019. Improved enrichment factor calculations through principal component analysis: examples from soils near breccia pipe uranium mines, Arizona, USA. Environ. Pollut. 248, 90–100. https://doi.org/10.1016/j.envpol.2019.01.122.

Bird, E.C.F., Dubois, J.-P., Iltis, J.A., 1984. The Impacts of Opencast Mining on the Rivers and Coasts of New Caledonia. The United Nations University. https://doi.org/10.1177/156482658100300205.

Boës, X., Rydberg, J., Martinez-Cortizas, A., Bindler, R., Renberg, I., 2011. Evaluation of conservative lithogenic elements (Ti, Zr, Al, and Rb) to study anthropogenic element enrichments in lake sediments. J. Paleolimnol. 46, 75–87. https://doi.org/10.1007/s10933-011-9515-z.

Brooks, T.M., Mittermeier, R.A., Da Fonseca, G.A.B., Gerlach, J., Hoffmann, M., Lamoreux, J.F., Mittermeier, C.G., Pilgrim, J.D., Rodrigues, A.S.L., 2006. Global biodiversity conservation priorities. Science 313, 58–61. https://doi.org/10.1126/science.1127609.

Brown, T.J., Hobbs, S.F., Idoine, N.E., Mills, A.J., Wrighton, C.E., Raycraft, E.R., 2016. World Mineral Production 2010-2014.

Bureau of Soils and Water Management, 2021. Land Use and Vegetation Maps. Department of Agriculture - BSWM Maps, Quezon City, Metro Manila.

Canadian Council of Ministers of the Environment, 2021. Canadian Environmental Quality Guidelines. Canadian Council of Ministers of the Environment - Guidelines.

Clemente, E.D., Domingo, S.N., Manejar, A.J.A., 2018. Answering Critical Questions on Mining in the Philippines. Philippine Institute for Development Studies - Discussion Paper Series No. 2018-38, Quezon City, Metro Manila.

Collins, A.L., Pulley, S., Foster, I.D.L., Gellis, A., Porto, P., Horowitz, A.J., 2017. Sediment source fingerprinting as an aid to catchment management: a review of the current state of knowledge and a methodological decision-tree for end-users. J. Environ. Manag. 194, 86–108. https://doi.org/10.1016/j.jenvman.2016.09.075.

Collins, A.L., Pulley, S., Foster, I.D.L., Gellis, A., Porto, P., Horowitz, A.J., 2016. Sediment source fingerprinting as an aid to catchment management: a review of the current state of knowledge and a methodological decision-tree for end-users. J. Environ. Manag. 194, 86–108. https://doi.org/10.1016/j.jenvman.2016.09.075.

Collins, A.L., Walling, D.E., 2002. Selecting fingerprint properties for discriminating potential suspended sediment sources in river basins. J. Hydrol. 261, 218–244. https://doi.org/10.1016/S0022-1694(02)00011-2.

Comber, S.D.W., Gunn, A.M., Whalley, C., 1995. Comparison of the partitioning of trace metals in the Humber and Mersey estuaries. Mar. Pollut. Bull. 30, 851–860. https://doi.org/10.1016/0025-326X(95)00092-2.

Commonwealth of Australia, 2019. Toxicant default guideline values for sediment quality [WWW Document]. Aust. New Zealand Guidel. Fresh Mar. Water Qual. URL. https://www.waterquality.gov.au/anz-guidelines/guideline-values/default/sediment-quality-toxicants, 8.25.21.

D'Haen, K., Verstraeten, G., Degryse, P., 2012. Fingerprinting historical fluvial sediment fluxes. Prog. Phys. Geogr. 36, 154–186. https://doi.org/10.1177/0309133311432581.

Dennis, I.A., Coulthard, T.J., Brewer, P., Macklin, M.G., 2009. The role of floodplains in attenuating contaminated sediment fluxes in formerly mined drainage basins. Earth Surf. Process. Landforms 34, 453–466. https://doi.org/10.1002/esp.1762.

Domingo, J.P.T., Attal, M., Mudd, S.M., Ngwenya, B.T., David, C.P.C., 2021. Seasonal fluxes and sediment routing in tropical catchments affected by nickel mining. Earth Surf. Process. Landforms 46, 2632–2655. https://doi.org/10.1002/esp.5198.

Domingo, L.E., Kyuma, K., 1983. Trace elements in tropical asian paddy soils: I. total trace element status. In: Soil Science and Plant Nutrition, pp. 439–452. https://doi.org/10.1080/00380768.1983.10434647.

Duodu, G.O., Goonetilleke, A., Ayoko, G.A., 2017. Potential bioavailability assessment, source apportionment and ecological risk of heavy metals in the sediment of Brisbane River estuary, Australia. Mar. Pollut. Bull. 117, 523–531. https://doi.org/10.1016/j.marpolbul.2017.02.017.

Feng, C., Guo, X., Yin, S., Tian, C., Li, Y., Shen, Z., 2017. Heavy metal partitioning of suspended particulate matter–water and sediment–water in the Yangtze Estuary. Chemosphere 185, 717–725. https://doi.org/10.1016/j.chemosphere.2017.07.075.

Gäbler, H.E., 1997. Mobility of heavy metals as a function of pH of samples from an overbank sediment profile contaminated by mining activities. J. Geochem. Explor. 58, 185–194. https://doi.org/10.1016/S0375-6742(96)00061-1.

Gaspar, L., Blake, W.H., Smith, H.G., Lizaga, I., Navas, A., 2019. Testing the sensitivity of a multivariate mixing model using geochemical fingerprints with artificial mixtures. Geoderma 337, 498–510. https://doi.org/10.1016/j.geoderma.2018.10.005.

Hakanson, L., 1980. An ecological risk index for aquatic pollution control.a sedimentological approach. Water Res. 14, 975–1001. https://doi.org/10.1016/0043-1354(80)90143-8.

Herzog, S.D., Persson, P., Kvashnina, K., Sofia Kritzberg, E., 2020. Organic iron complexes enhance iron transport capacity along estuarine salinity gradients of Baltic estuaries. Biogeosciences 17, 331–344. https://doi.org/10.5194/bg-17-331-2020.

Hin, J.A., Osté, L.A., Schmidt, C.A., 2010. Guidance document for sediment assessment. Minist. Infrastruct. Environ. - DG Water 1–153.

Holden, W.N., 2015. Mining amid typhoons: large-scale mining and typhoon vulnerability in the Philippines. Extr. Ind. Soc. 2, 445–461. https://doi.org/10.1016/j.exis.2015.04.009.

Horowitz, A.J., 1991. A primer on sediment-trace element chemistry. U.S. Geol. Surv. Open-File Rep. 1–136.

Hu, B., Li, J., Bi, N., Wang, H., Yang, J., Wei, H., Zhao, J., Li, G., Yin, X., Liu, M., Zou, L., Li, S., 2015. Seasonal variability and flux of particulate trace elements from the Yellow River: impacts of the anthropogenic flood event. Mar. Pollut. Bull. 91, 35–44. https://doi.org/10.1016/j.marpolbul.2014.12.030.

Idoine, N.E., Raycraft, E.R., Shaw, R.A., Hobbs, S.F., Deady, E.A., Everett, P., Evans, E.J., Mills, A.J., 2022. World Mineral Production 2016–2020. British Geological Survey.

Jalowska, A.M., McKee, B.A., Laceby, J.P., Rodriguez, A.B., 2017. Tracing the sources, fate, and recycling of fine sediments across a river-delta interface. Catena 154, 95–106. https://doi.org/10.1016/j.catena.2017.02.016.

Jung, H.B., Yun, S.T., Mayer, B., Kim, S.O., Park, S.S., Lee, P.K., 2005. Transport and sediment-water partitioning of trace metals in acid mine drainage: an example from the abandoned Kwangyang Au-Ag mine area, South Korea. Environ. Geol. 48, 437–449. https://doi.org/10.1007/s00254-005-1257-7.

Ke, X., Gui, S., Huang, H., Zhang, H., Wang, C., Guo, W., 2017. Ecological risk assessment and source identification for heavy metals in surface sediment from the Liaohe River protected area, China. Chemosphere 175, 473–481. https://doi.org/10.1016/j.chemosphere.2017.02.029.

Kjelland, M.E., Woodley, C.M., Swannack, T.M., Smith, D.L., 2015. A review of the potential effects of suspended sediment on fishes: potential dredging-related physiological, behavioral, and transgenerational implications. Environ. Syst. Decis. 35, 334–350. https://doi.org/10.1007/s10669-015-9557-2.

Król, A., Mizerna, K., Bożym, M., 2020. An assessment of pH-dependent release and mobility of heavy metals from metallurgical slag. J. Hazard Mater. 384, 1–9. https://doi.org/10.1016/j.jhazmat.2019.121502.

Laceby, J.P., Gellis, A.C., Koiter, A.J., Blake, W.H., Evrard, O., 2019. Preface — evaluating the response of critical zone processes to human impacts with sediment source fingerprinting. J. Soils Sediments 19, 3245–3254. https://doi.org/10.1007/s11368-019-02409-0.

Lecce, S.A., Pavlowsky, R.T., 2014. Floodplain storage of sediment contaminated by mercury and copper from historic gold mining at Gold Hill, North Carolina, USA. Geomorphology 206, 122–132. https://doi.org/10.1016/j.geomorph.2013.10.004.

Lizaga, I., Latorre, B., Gaspar, L., Navas, A., 2020. FingerPro: an R Package for tracking the provenance of sediment. Water Resour. Manag. 34, 3879–3894. https://doi.org/10.1007/s11269-020-02650-0.
MacDonald, D.D., Ingersoll, C.G., Berger, T.A., 2000. Development and evaluation of consensus-based sediment quality guidelines for freshwater ecosystems. Arch. Environ. Contam. Toxicol. 39, 20–31. https://doi.org/10.1007/s002440010075.
Macklin, M.G., Brewer, P.A., Hudson-Edwards, K.A., Bird, G., Coulthard, T.J., Dennis, I. A., Lechler, P.J., Miller, J.R., Turner, J.N., 2006. A geomorphological approach to the management of rivers contaminated by metal mining. Geomorphology 79, 423–447. https://doi.org/10.1016/j.geomorph.2006.06.024.
Magahud, J.C., Badayos, R.B., Sanchez, P.B., Sta Cruz, P.C., 2015. Levels and potential sources of heavy metals in major irrigated rice areas of the Philippines. IAMURE Int. J. Ecol. Conserv. 15, 28–59. https://doi.org/10.7718/ijec.v15i1.1000.
Malvandi, H., 2017. Preliminary evaluation of heavy metal contamination in the Zarrin-Gol River sediments, Iran. Mar. Pollut. Bull. 117, 547–553. https://doi.org/10.1016/j.marpolbul.2017.02.035.
McIntyre, N., Bulovic, N., Cane, I., McKenna, P., 2016. A multi-disciplinary approach to understanding the impacts of mines on traditional uses of water in Northern Mongolia. Sci. Total Environ. 557–558, 404–414. https://doi.org/10.1016/j.scitotenv.2016.03.092.
McKay, M.D., Beckman, R.J., Conover, W.J., 1979. A comparison of three methods for selecting values of input variables in the analysis of output from a computer code. Technometrics 42, 55–61. https://doi.org/10.1080/00401706.2000.10485979.
McLaren, J., Beauchemin, D., Berman, S., 1987. Determination of trace metals in marine sediments by inductively coupled plasma mass spectrometry. J. Anal. At. Spectrom. 277–281.
McLaren, J., Berman, S.S., Boyko, V.J., Russell, D.S., 1981. Simultaneous determination of major, minor, and trace elements in marine sediments by inductively coupled plasma atomic emission spectrometry. Anal. Chem. 1802–1806.
Messina, A.M., Biggs, T.W., 2016. Contributions of human activities to suspended sediment yield during storm events from a small, steep, tropical watershed. J. Hydrol. 538, 726–742. https://doi.org/10.1016/j.jhydrol.2016.03.053.
Migo, V.P., Mendoza, M.D., Alfafara, C.G., Pulhin, J.M., 2018. Water Policy in the Philippines - Issues, Initiatives, and Prospects. In: Industrial Water Use and the Associated Pollution and Disposal Problems in the Philippines, Global Issues in Water Policy, vol. 8. Springer International Publishing. https://doi.org/10.1007/978-3-319-70969-7.
Miller, J.R., Mackin, G., Orbock Miller, S.M., 2015. Geochemical fingerprinting. In: Application of Geochemical Tracers to Fluvial Sediment, pp. 11–51. https://doi.org/10.1007/978-3-319-13221-1.
Miller, J.R., Miller, S.M.O., 2007. Contaminated Rivers: A Geomorphological-Geochemical Approach to Site Assessment and Remediation, Contaminated Rivers. Springer, Dordrecht, The Netherlands. https://doi.org/10.1007/1-4020-5602-8.
Mines and Geosciences Bureau, 2022. Mining Tenements Statistics Report for Month of May 2022: Mineral Production Sharing Agreement (MPSA).
Mora, A., Mahlknecht, J., Baquero, J.C., Laraque, A., Alfonso, J.A., Pisapia, D., Balza, L., 2017. Dynamics of dissolved major (Na, K, Ca, Mg, and Si) and trace (Al, Fe, Mn, Zn, Cu, and Cr) elements along the lower Orinoco River. Hydrol. Process. 31, 597–611. https://doi.org/10.1002/hyp.11051.
Nasrabadi, T., Ruegner, H., Sirdari, Z.Z., Schwientek, M., Grathwohl, P., 2016. Using total suspended solids (TSS) and turbidity as proxies for evaluation of metal transport in river water. Appl. Geochem. 68, 1–9. https://doi.org/10.1016/j.apgeochem.2016.03.003.
Nordstrom, D.K., Ball, J.W., 1986. The geochemical behavior of aluminum in acidified surface waters. Science 232, 54–56. https://doi.org/10.1126/science.232.4746.54.
Nosrati, K., Collins, A.L., 2019a. Fingerprinting the contribution of quarrying to fine-grained bed sediment in a mountainous catchment, Iran. River Res. Appl. 35, 290–300. https://doi.org/10.1002/rra.3408.
Nosrati, K., Collins, A.L., 2019b. Investigating the importance of recreational roads as a sediment source in a mountainous catchment using a fingerprinting procedure with different multivariate statistical techniques and a Bayesian un-mixing model. J. Hydrol. 569, 506–518. https://doi.org/10.1016/j.jhydrol.2018.12.019.
Nosrati, K., Collins, A.L., Madankan, M., 2018. Fingerprinting sub-basin spatial sediment sources using different multivariate statistical techniques and the Modified MixSIR model. Catena 164, 32–43. https://doi.org/10.1016/j.catena.2018.01.003.
Palazón, L., Latorre, B., Gaspar, L., Blake, W.H., Smith, H.G., Navas, A., 2015. Comparing catchment sediment fingerprinting procedures using an auto-evaluation approach with virtual sample mixtures. Sci. Total Environ. 532, 456–466. https://doi.org/10.1016/j.scitotenv.2015.05.003.
Palazón, L., Navas, A., 2017. Variability in source sediment contributions by applying different statistic test for a Pyrenean catchment. J. Environ. Manag. 194, 42–53. https://doi.org/10.1016/j.jenvman.2016.07.058.
Pekey, H., 2006. The distribution and sources of heavy metals in Izmit Bay surface sediments affected by a polluted stream. Mar. Pollut. Bull. 52, 1197–1208. https://doi.org/10.1016/j.marpolbul.2006.02.012.
Philippine Senate Blue Ribbon Committee, 2017. Committee Report No. 197. Pasay City.
Pluta, B., 2006. EPA Region III BTAG -Freshwater Sediment Screening Benchmarks.
Pulley, S., Foster, I., Antunes, P., 2015. The uncertainties associated with sediment fingerprinting suspended and recently deposited fluvial sediment in the Nene river basin. Geomorphology 228, 303–319. https://doi.org/10.1016/j.geomorph.2014.09.016.
Ramos-Scharrón, C.E., MacDonald, L.H., 2007. Measurement and prediction of natural and anthropogenic sediment sources. St. John, U.S. Virgin Islands. Catena 71, 250–266. https://doi.org/10.1016/j.catena.2007.03.009.
Risk, M.J., 2014. Assessing the effects of sediments and nutrients on coral reefs. Curr. Opin. Environ. Sustain. 7, 108–117. https://doi.org/10.1016/j.cosust.2014.01.003.
Sellier, V., Navratil, O., Laceby, J.P., Allenbach, M., Lefèvre, I., Evrard, O., 2020. Investigating the use of fallout and geogenic radionuclides as potential tracing properties to quantify the sources of suspended sediment in a mining catchment in New Caledonia , South Pacific. J. Soil. Sediments 20, 1112–1128.
Senate of the Philippines, 2014. Senate Resolution No. 547. Philippines.
Sheppard, S., Long, J., Sanipelli, B., Sohlenius, G., 2009. Solid/liquid Partition Coefficients (Kd) for Selected Soils and Sediments at Forsmark and Laxemar-Simpevarp. Svensk Kärnbränslehantering AB (SKB), Stockholm.
Singer, M.B., Harrison, L.R., Donovan, P.M., Blum, J.D., Marvin-DiPasquale, M., 2016. Hydrologic indicators of hot spots and hot moments of mercury methylation potential along river corridors. Sci. Total Environ. 568, 697–711. https://doi.org/10.1016/j.scitotenv.2016.03.005.
Stock, J.D., Rosener, M., Schmidt, K.M., Hanshaw, M.N., Brooks, B., Tribble, G., Jacobi, J., 2010. Sediment Budget for a Polluted Hawaiian Reef Using Hillslope Monitoring and Process Mapping. American Geophysical Union. Fall Meeting 2010 (Abstract).
Sutherland, R.a., 2000. Bed sediment-associated trace metals in an urban stream, Oahu, Hawaii. Environ. Geol. 39, 611–627. https://doi.org/10.1007/s002540050473.
The European Parliament and the Council of the European Union, 2008. Directive 2008/105/EC of the European Parliament and of the Council of 16 December 2008 on Environmental Quality Standards in the Field of Water Policy. Official Journal of the European Union.
US Environmental Protection Agency, 1999. Understanding Variation in Partition Coefficient, Kd, Values, vol. I. The Kd Model, Methods of Measurement, and Application of Chemical Reaction Codes, USEPA.
US Environmental Protection Agency, 2014. Priority pollutant list. Washington, D.C.
US National Oceanic and Atmospheric Administration, 1999. Sediment Quality Guidelines Developed for the National Status and Trends Program.
Varol, M., 2011. Assessment of heavy metal contamination in sediments of the Tigris River (Turkey) using pollution indices and multivariate statistical techniques. J. Hazard Mater. 195, 355–364. https://doi.org/10.1016/j.jhazmat.2011.08.051.
Walling, D.E., Collins, A.L., 2016. Fine sediment transport and management Background and context. In: Gilvear, D.J., Greenwood, M.T., Thoms, M.C., Wood, P.J. (Eds.), River Science: Research and Management for the 21st Century. John Wiley & Sons, Ltd., pp. 37–60
Wen, Y., Yang, Z., Xia, X., 2013. Dissolved and particulate zinc and nickel in the Yangtze River (China): distribution, sources and fluxes. Appl. Geochem. 31, 199–208. https://doi.org/10.1016/j.apgeochem.2013.01.004.
Yang, Z., Xia, X., Wang, Y., Ji, J., Wang, D., Hou, Q., Yu, T., 2014. Dissolved and particulate partitioning of trace elements and their spatial-temporal distribution in the Changjiang River. J. Geochem. Explor. 145, 114–123. https://doi.org/10.1016/j.gexplo.2014.05.013.
Yavar Ashayeri, N., Keshavarzi, B., 2019. Geochemical characteristics, partitioning, quantitative source apportionment, and ecological and health risk of heavy metals in sediments and water: a case study in Shadegan Wetland, Iran. Mar. Pollut. Bull. 149, 1–16. https://doi.org/10.1016/j.marpolbul.2019.110495.
Zapico, I., Laronne, J.B., Martín-Moreno, C., Martín-Duque, J.F., Ortega, A., Sánchez-Castillo, L., 2017. Baseline to evaluate off-site suspended sediment-related mining effects in the Alto tajo natural Park, Spain. L. Degrad. Dev. 28, 232–242. https://doi.org/10.1002/ldr.2605.
Zhang, Z., Lu, Y., Li, H., Tu, Y., Liu, B., Yang, Z., 2018. Assessment of heavy metal contamination, distribution and source identification in the sediments from the Zijiang River, China. Sci. Total Environ. 645, 235–243. https://doi.org/10.1016/j.scitotenv.2018.07.026.
Zhao, S., Feng, C., Wang, D., Liu, Y., Shen, Z., 2013. Salinity increases the mobility of Cd, Cu, Mn, and Pb in the sediments of Yangtze Estuary: relative role of sediments' properties and metal speciation. Chemosphere 91, 977–984. https://doi.org/10.1016/j.chemosphere.2013.02.001.